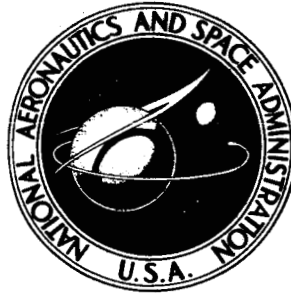


~~RESTRICTED DATA~~
ATOMIC ENERGY ACT OF 1954

**NASA TECHNICAL
MEMORANDUM**



UB
NASA TM X-1450

NOV 09 2004

LIBRARY COPY

OCT 4 1967

LEWIS LIBRARY, NASA
CLEVELAND, OHIO

**THERMAL CYCLIC STABILITY
OF CLAD CERMETS PREPARED
FROM TUNGSTEN-COATED
URANIUM DIOXIDE PARTICLES**

by Philip D. Takkunen and Robert J. Baker

*Lewis Research Center
Cleveland, Ohio*

CLASSIFICATION CHANGED

To Unclassified

By authority of H. H. Mairis

Date Jan. 3, 1973
per lmd

THERMAL CYCLIC STABILITY OF CLAD CERMETS PREPARED FROM
TUNGSTEN-COATED URANIUM DIOXIDE PARTICLES

By Philip D. Takkunen

Lewis Research Center
Cleveland, Ohio

and

Robert J. Baker

Battelle Memorial Institute
at the Atomic Energy Commission's
Pacific Northwest Laboratories
Richland, Washington

~~RESTRICTED DATA~~

ATOMIC ENERGY ACT OF 1954

~~GROUP 1
Excluded from automatic
downgrading and declassification~~

CLASSIFIED DOCUMENT—TITLE UNCLASSIFIED

This material contains information affecting the national defense of the United States within the meaning of the espionage laws, Title 18, U.S.C., Secs. 793 and 794, the transmission or revelation of which in any manner to an unauthorized person is prohibited by law.


NOTICE

This document should not be returned after it has satisfied your requirements. It may be disposed of in accordance with your local security regulations or the appropriate provisions of the Industrial Security Manual for Safe-Guarding Classified Information.

NATIONAL AERONAUTICS AND SPACE ADMINISTRATION

CONTENTS

	Page
SUMMARY	1
INTRODUCTION	2
EXPERIMENTAL PROCEDURES	3
Specimen Preparation	3
Test Procedures	4
RESULTS	5
Effect of Cermet Quality on Fuel Loss	5
Effect of Hydrogen Pressure	5
Effect of Peak Cycling Temperature	6
Effect of Time at Temperature per Cycle	6
Dimensional Growth	7
Fracturing and Blistering	7
DISCUSSION	8
Characterization of Fuel Migration and Loss	8
Effect of Specimen Defects	9
Effects of Cycling Conditions	10
Hydrogen pressure	10
Peak cycling temperature and time at temperature per cycle in high-pressure hydrogen	11
CONCLUDING REMARKS	12
SUMMARY OF RESULTS	12
APPENDIX - TRANSIENT PRESSURE EFFECT	14
REFERENCES	16



THERMAL CYCLIC STABILITY OF CLAD CERMETS PREPARED FROM TUNGSTEN-COATED URANIUM DIOXIDE PARTICLES (U)

by Philip D. Takkunen and Robert J. Baker*

Lewis Research Center


SUMMARY

Thermal cyclic induced fuel loss from fueled cermets composed of uranium dioxide (UO_2) particles dispersed in a tungsten matrix has been one of the major material problems encountered in a feasibility study of the NASA tungsten, water-moderated nuclear rocket concept. In this study, cermet specimens were fabricated by hot isostatic consolidation of tungsten-coated UO_2 (nominally W-35-volume-percent UO_2 containing 18-mole-percent cerium oxide (CeO_2) or 10-mole-percent yttrium oxide (Y_2O_3) in the UO_2 particles followed by complete encapsulation of the consolidated cermets with vapor deposited tungsten. These specimens were tested under a variety of thermal cycling conditions.

The results showed that cermets containing either CeO_2 or Y_2O_3 in the UO_2 lost less than 1 weight percent of their fuel after twenty five 10-minute cycles to 2500°C in 15 or 600 psia (0.10 or 4.1 MN/m^2) of dry, flowing hydrogen. Thermal cycling in 600 psia (4.1 MN/m^2) of hydrogen, however, produced blisters and gross fractures in some cermets; these phenomena were not observed in any cermets cycled in 15 psia (0.10 MN/m^2) of hydrogen. An increase in either time at temperature per cycle (60 and 120 min) or cycling temperature (to 2600°C) resulted in increased fuel loss after a given number of cycles in hydrogen at either pressure. The combined cycling conditions of 2600°C and 600 psia (4.1 MN/m^2) of hydrogen caused catastrophic fuel loss and gross fracturing of cermets after only 5 to 15 thermal cycles.

The large degree of fuel loss scatter observed between specimens at all cycling conditions is indicative of uncontrolled variables in cermet fabrication. These variables must be controlled to ensure the reliable and consistent thermal cyclic fuel retention performance of fuel elements in a nuclear rocket.

* Battelle Memorial Institute at the Atomic Energy Commission's Pacific Northwest Laboratories.



INTRODUCTION

A major portion of the previous materials work for the NASA tungsten, water-moderated nuclear rocket concept (TWMR, ref. 1) has centered on the fabrication and compatibility of cermets for fuel elements. These cermets, which consist of uranium dioxide (UO_2) particles dispersed in a tungsten matrix, have been demonstrated to lose fuel via volatilization at temperatures expected to be reached during rocket operation, that is, 2500°C (ref. 2). This fuel loss was shown to be greatly accelerated when cermets were thermally cycled in flowing hydrogen (refs. 2 to 4) as would be required during nuclear rocket preflight tests and operational restarts.

Volatilization of UO_2 under static (noncyclic) thermal treatments at 2500°C was effectively eliminated by (1) coating each UO_2 particle with tungsten via vapor deposition prior to consolidation into cermets (ref. 5) and (2) cladding the exterior surfaces of consolidated cermets with tungsten via vapor deposition (ref. 6). Elongation of fuel particles, which occurs in some consolidation processes, such as hot rolling or extrusion, may also contribute to fuel loss because the probability of particle interconnection is increased. Fuel particle elongation was essentially eliminated in this study by utilizing hot isostatic compaction as the method of consolidation. This consolidation method causes no significant particle elongation and has the added advantage of being capable of consolidating cermets into complex geometries such as the proposed honeycomb-type fuel element configuration discussed in reference 7.

The problem of fuel loss resulting from thermal cycling has proven to be much more complex in nature. References 3, 4, and 8 have shown that the most effective method of reducing thermal cyclic induced fuel decomposition, migration, and loss is the addition of metal oxides to UO_2 in solid solution. Reference 9 reported that, of 13 metal oxides studied, cerium oxide and yttrium oxide were two of the more effective oxides in reducing fuel loss.

Prior to this investigation, no comprehensive study had been conducted on the behavior during thermal cycling of fully clad (with tungsten) specimens fabricated by hot isostatic compaction of tungsten-coated UO_2 particles which contained metal oxide additives. Therefore, it was the purpose of this investigation to study the behavior of specimens of this type under varying thermal cyclic conditions and to determine if these specimens could meet a fuel loss goal of less than 1-weight-percent UO_2 loss after 25 thermal cycles to 2500°C in a flowing hydrogen atmosphere. Specimens were subjected to thermal cycling peak temperatures of either 2500°C or 2600°C and times at temperature per cycle from 10 to 120 minutes in flowing (35 standard cu ft/hr ($1.0\text{ m}^3/\text{hr}$)) dry hydrogen at either 15 or 600 psia (0.10 or 4.1 MN/m^2 which will hereafter be called "low" or "high" pressure). Special emphasis was put on determination of the effects of high-pressure hydrogen testing because this pressure simulates the expected rocket operating condition and

CONFIDENTIAL

because other work has indicated possible detrimental effects at high pressure (refs. 9 and 10).

All specimens were fabricated with a 35-volume-percent UO_2 loading since, in the fuel loading range of interest for the TWMR concept (10 to 35 percent), the highest loading was shown to be the most critical with respect to fuel loss (ref. 4). The UO_2 contained either 18-mole-percent cerium oxide (CeO_2) or 10-mole-percent yttrium oxide (Y_2O_3). Specimens were characterized before and after thermal cycling by metallography, radiography, visual observation, weight loss, and dimensional growth. The results of these observations are reported and discussed in this paper.

EXPERIMENTAL PROCEDURES

Specimen Preparation

Specimens tested in this study were fabricated as illustrated in the process flow diagram of figure 1 incorporating the following major steps:

- (1) Solid solution and spherical fuel particle preparation;
- (2) Tungsten coating of the particles by vapor deposition;
- (3) Consolidation of the particles into plates by hot isostatic compaction; and
- (4) Tungsten vapor deposition cladding of the cermet surfaces.

The spherical particles which were prepared by a coprecipitation and agglomeration process contained nominally 18 mole percent of CeO_2 and 10 mole percent of Y_2O_3 in the UO_2 . (See table I for chemical and physical analyses.) These concentration levels were chosen to permit comparisons of the effectiveness of additives at equivalent oxide cation to uranium atom ratios (i. e., for 18-mole-percent CeO_2 and 10-mole-percent Y_2O_3 in UO_2 , $\text{Ce}/\text{U} \cong \text{Y}/\text{U} \cong 0.22$). In addition, these additive concentration levels had previously been shown (refs. 8 and 9) to adequately stabilize W- UO_2 cermets without unduly increasing the ceramic content of the cermets. (See ref. 11 for the effect of ceramic content on the strength of W- UO_2 cermets.)

X-ray diffraction patterns indicated that only fluorite (FCC) crystal structures were present in the particles containing either additive. (See table I for lattice parameters.) Metallographic analysis, however, revealed a ceramic-appearing second phase (fig. 2(a)) in some of the UO_2 particles containing CeO_2 . This second phase is believed to be CeO_2 which did not go into solid solution. This phase was only rarely observed after hot isostatic consolidation or thermal cycling of cermets and was not observed to have any effect upon the behavior of cermets in this study. Other than this phase, all the photomicrographs in figure 2 are typical of cermets containing either Y_2O_3 or CeO_2 . Close examination of the particle microstructures also revealed a very small metallic -

CONFIDENTIAL

appearing phase which is thought to be tungsten (as will be discussed later).

After the particles were classified, they were coated with tungsten to achieve the desired 35-volume-percent UO_2 loading. (See table I for analyzed UO_2 loading.) The coating process consisted of first vapor depositing a very thin layer (about 2 to 3 μm) by hydrogen reduction of WCl_6 and then vapor depositing the remainder of the coating thickness by hydrogen reduction of WF_6 . The initial WCl_6 -produced coating was used in an effort to reduce fluoride contamination which may have a detrimental effect on the thermal cyclic behavior of cermets (ref. 5). The impurity levels of fluorine and several other elements in the particles before and after they were tungsten coated are listed in table I. In addition, table I gives the densities of the particles before and after coating.

The coated particles were packed in a molybdenum can and isostatically consolidated at 30 000 psi (200 MN/m^2) and 1650° C for 2 hours using the procedures reported in references 7 and 12. The microstructure of a consolidated cermet (fig. 2(b)) illustrates the degree of particle sphericity maintained and the high cermet density achieved. According to water immersion density tests (table I), the cermet density was over 98 percent of theoretical. The molybdenum cans then were leached away from the W- UO_2 cermet plates, and the plates were cut to specimen size (1 by 1 by 0.020 in. (2.5 by 2.5 by 0.05 cm)) with a water-cooled cutoff wheel. The microstructure of a specimen (fig. 2(c)) illustrates the typically jagged cermet surfaces resulting from leaching surface UO_2 particles.

The final step in the fabrication process was vapor deposition of tungsten onto cermet surfaces by hydrogen reduction of WCl_6 . The cermets were completely encapsulated with a 25 to 50 μm thick layer of tungsten utilizing procedures reported in reference 6. A typical microstructure (fig. 2(d)) shows notches and cavities in the cladding which resulted from the vapor deposited tungsten following the contours of the jagged substrate (fig. 2(c)) left from the leaching process.

Test Procedures

Two furnaces were utilized in this study to enable testing at both 15 and 600 psia (0.10 and 4.1 MN/m^2). All of the high-pressure tests and some of the low-pressure tests were accomplished at the Pacific Northwest Laboratory, Battelle Memorial Institute (BNW), under contract to NASA. These tests were conducted in an all-metal furnace which employed a tungsten mesh resistance heating element (ref. 10). Most of the low-pressure studies were done at the Lewis Research Center, NASA, in a zirconium oxide (ZrO_2) insulated, induction-heated furnace which is described in reference 13. Table II gives a detailed comparison of the operating characteristics of the furnaces. Because of the similar operating characteristics and the similar behavior of cermets cycled in either furnace at low pressure, data from both furnaces are used interchangeably throughout this report.

[REDACTED]

After thermal cycling, the specimens were characterized by measuring fuel loss (weight loss as a percent of the original UO_2 content), by measuring the growth in specimen thickness, and by examining the specimens metallographically, radiographically, and visually.

RESULTS

Effect of Cermet Quality on Fuel Loss

Defects originating in cermets during fabrication appeared to have a considerable effect on cermet behavior during thermal cycling. This behavior is illustrated (fig. 3) by the scatter in fuel loss data from similar cermets cycled to 2500°C in low-pressure hydrogen. Scatter in fuel loss data was observed for cermets at each set of cycling conditions used and, in general, appeared more pronounced in cermets cycled in high-pressure hydrogen.

The presence of flaws in the cladding was found to correlate with fuel loss from cermets. A qualitative examination of specimens prepared for metallography revealed that those specimens which exhibited the greatest degree of fuel retention also exhibited the least number of cladding notches and cavities. The effects of other fabrication variables, such as impurity contents and variations in cladding quality and thickness, were not quantitatively determined. Unfortunately, elimination of specimens with cladding defects was not possible prior to testing because adequate nondestructive testing methods were not available.

Because of the limited number of specimens available for testing and because of the scatter in data, only the "best" curves (lowest rate of fuel loss) achieved thus far are presented in this report. While comparisons based on these curves are tentative, the curves illustrate the potential of these cermets for retaining fuel under the varying cycling conditions studied. If all fabrication defects were eliminated, fuel retention properties could conceivably be increased over those reported in this paper since the best specimens studied also had observable defects. In addition to the fuel loss curves, pertinent metallographic, radiographic, and visual observations on specimens tested are presented in order to aid in understanding the fuel loss curves. The presentation of these observations is not confined to the best specimens.

Effect of Hydrogen Pressure

The effect of increasing hydrogen pressure on fuel loss is shown in figure 4. Neither the hydrogen pressure nor the type of additive (CeO_2 or Y_2O_3) in the cermets had any

[REDACTED]

[REDACTED]

significant effect on fuel loss through 50 cycles to 2500⁰ C. The reactor goal of less than 1 percent of loss after 25 cycles was attained at either hydrogen pressure.

Figure 5 illustrates the microstructures of cermets (whose fuel loss curves are shown in fig. 4) after 50 thermal cycles. While fuel migration along grain boundaries was minor in those cermets cycled in low-pressure hydrogen and the cermet containing CeO₂ cycled in high-pressure hydrogen, a considerable degree of fuel migration was observed in the Y₂O₃ containing cermet cycled in high-pressure hydrogen. The resulting increased interconnection of fuel particles would be expected to result in much greater fuel loss should the cladding rupture. Note also the internal porosity which developed in the tungsten matrix of all these specimens during thermal cycling. The causes and implications of this porosity will be discussed later.

Effect of Peak Cycling Temperature

Comparing figure 4 with figure 6 shows that increasing the cycling temperature from 2500⁰ to 2600⁰ C resulted in increased fuel loss from cermets cycled at either hydrogen pressure. For cermets containing either additive, the high-pressure tests at 2600⁰ C resulted in rapidly accelerating fuel loss after a lower number of thermal cycles than did the low-pressure tests. The accelerated fuel loss at high pressure was accompanied by increased fuel migration and by internal cracking, gross fracturing, and deterioration of the cermets.

Figure 6 indicates that CeO₂ was more effective in reducing fuel loss from cermets cycled to 2600⁰ C in low-pressure hydrogen than was Y₂O₃, but this effectiveness was reversed in high-pressure testing. Since all of these specimens exhibited some cladding defects, the relative effectiveness of the CeO₂ and the Y₂O₃ additives may have been obscured. Further work should be done on defect-free or controlled-defect specimens in order to determine which additive is more effective in reducing fuel loss.

Effect of Time at Temperature per Cycle

Figures 7(a) and (b) show the effect of variations in the time at temperature (2500⁰ C) per cycle on fuel loss in hydrogen at low and high pressure, respectively. The fuel-loss curves indicate that at either pressure, and with either additive, increasing the time at temperature per cycle from 10 to 60 minutes resulted in a decreasing number of cycles before an equal amount of fuel was lost. We observed, however, that fuel migration was more extensive in cermets cycled in high than in low pressure. Increasing the time per cycle still further from 60 to 120 minutes in the low-pressure tests (this test was not run

CONFIDENTIAL

at high pressure) resulted in very little change in the fuel-loss curves from 60-minute cycles. Cermets containing CeO_2 exhibited greater fuel retention and less fuel migration than cermets containing Y_2O_3 for cycles longer than 10 minutes in either low- or high-pressure hydrogen. Table III summarizes the fuel loss curves by listing the number of cycles and the accumulated time at temperature resulting in 2-weight-percent fuel loss from cermets for each of the times at 2500°C per cycle tested. The accumulated time at temperature resulting in 2-weight-percent fuel loss was found to increase with increasing time at temperature per cycle for cermets cycled in low-pressure hydrogen. On the other hand, no change in the accumulated time at temperature with increased time at temperature per cycle was observed in cermets cycled in high-pressure hydrogen. It should be emphasized that all the results given in this table represent only a few specimens and, therefore, should be interpreted qualitatively. The value of such a table, however, is readily apparent when considering a rocket mission and predicting fuel element life.

Dimensional Growth

Linear dimensional growth of W- UO_2 cermets containing CeO_2 and Y_2O_3 during thermal cycling has been observed previously on plate-type specimens (ref. 9). Measurements of the growth in thickness of the plate specimens tested in this study are plotted in figure 8. While some scatter in measurements was found, the rate of thickness growth was calculated to be approximately 0.1 percent per cycle irrespective of the cycling conditions used or the type of additive in the UO_2 . This growth rate was less than half that previously reported for specimens with the same composition but fabricated by powder metallurgical techniques and employing very thick (0.2 in. (0.5 cm)) tungsten edge claddings (ref. 9). It is hypothesized that the thick cladding constrained growth in all but the thickness direction in the previously tested specimens and therefore increased the rate of growth in thickness. Further work should be done, however, to determine reasons for the difference in growth rates.

Fracturing and Blistering

Numerous fractures and blisters were found in those cermets cycled in high-pressure hydrogen. A summary of the frequency of these is shown in table IV. None of these faults were found in cermets cycled in low-pressure hydrogen. An increase in time at temperature per cycle and, to a greater extent, an increase in cycling temperature in high-pressure hydrogen resulted in an increasing frequency of specimens exhibiting fractures. These cycling conditions, however, had no effect on the frequency of

CONFIDENTIAL

specimens exhibiting blisters. Possible reasons for cermet fracturing the blistering are discussed later in this report.

Typical illustrations of internal cracking and surface fracturing in cermets are shown in figure 9. Internal cracking was observed in some cermets exhibiting relatively extensive fuel migration, but relatively low fuel loss (figs. 9(a) and (b)). Surface fractures became apparent (fig. 9(c)) concomitant with extensive fuel migration and accelerated fuel loss.

Macrographs of cermets exhibiting blisters, which were generally located near the cermet edges, are shown in figures 10(a) and (b). In contrast to fractures, blisters appeared in cermets before the fuel loss began to rapidly accelerate and before extensive fuel migration had occurred. Blisters were observed both within the cermet core (fig. 10(a)) and at the cermet-cladding interface (fig. 10(b)). An interesting observation to be made in figure 10 is the nearly continuous layer of fuel along the internal surface of each blister. It is believed that this layer is composed of exposed fuel particles and of fuel transported, via the vapor phase, to these internal surfaces. No fuel was observed to be lost from the blisters during thermal cycling unless the blister was broken during handling.

DISCUSSION

Characterization of Fuel Migration and Loss

The mechanisms of fuel loss and of UO_2 stabilization by metal oxides to reduce fuel loss upon thermal cycling are discussed in detail in references 8 and 9. Briefly, fuel deterioration was hypothesized to result from decomposition of the UO_2 into a substoichiometric state which, upon cooling, disproportionates to give free uranium. The uranium (or a uranium-rich species) is then free to migrate throughout the tungsten matrix until it is exposed to the atmosphere and volatilized.

Typical examples of fuel migration along grain boundaries in coated-particle cermets are exhibited in figure 11. Figure 11(a), which shows a microstructure typical of initial fuel migration, illustrates fuel "nubs" which project out from the originally spherical fuel particles. In addition, some of the tungsten matrix microvoids, which developed in all the cermets during thermal cycling, are observed to contain some migrated fuel.

Figure 11(b) illustrates a cermet in which more extensive fuel migration had occurred than in the cermet shown in figure 11(a). Migrated fuel between fuel particles and from the particles through the cladding to the external surface of the cermet can be observed along tungsten grain boundaries in figure 11(b). This interconnection of particles and development of channels through a cladding by fuel migration is believed to be

[REDACTED]

one of the major factors leading to rapid fuel loss. It is also interesting to note the spherical appearance of the migrated fuel in the grain boundaries of the tungsten matrix and cladding. This phenomenon may be due to spherical voids in the cermet which are filled with migrated fuel or to solidification of a molten, migrating specie.

Addition of metal oxides, such as CeO_2 and Y_2O_3 , in solid solution with UO_2 decreases the rate of fuel decomposition and, thus, fuel migration and fuel loss (ref. 9). Although these additives delayed fuel migration in specimens tested in this study, they did not eliminate it. The serrated surfaces of fuel particles exhibited in figure 11(c) are believed to represent areas where fuel decomposition had occurred and from which fuel had migrated.

Fuel microporosity and a small amount of metallic appearing phase (identified as tungsten by electron microprobe analysis) were observed in the interior of fuel particles (fig. 11(d)) after thermal cycling. This phenomenon was randomly observed in cycled cermets and could not be related to a particular cycling condition. The fuel microporosity is believed to originate from the original porosity found in the coated particles (fig. 2(a)). After hot isostatic consolidation, the porosity apparently became too fine to be detected at ordinary magnifications (fig. 2(b)). These pores are believed to have coalesced in the center of some fuel particles during thermal cycling. The tungsten observed in the fuel particles is believed to have been deposited in the pores of particles during vapor deposition cladding of the particles (fig. 2(a)). Further work should be done to determine the mechanisms and implications of this phenomenon. For example, control of fuel particle porosity formation may provide a means of accommodating fission gas products from a nuclear reaction.

Effect of Specimen Defects

Defects in specimens resulting directly and/or indirectly from fabrication are believed to have an important effect on their thermal cyclic behavior. The major defects observed were (1) microvoids in the tungsten matrix (fig. 5) which were generated during thermal cycling and (2) notches, cavities, and voids present in the "as-fabricated" cermet claddings (fig. 2). Other defects such as impurities at the cermet-cladding interface or in the cermet cladding may have also affected the behavior of specimens during thermal cycling.

Microvoids were formed in the matrix of the cermet core after only a few thermal cycles regardless of cycling conditions (figs. 5, 9, and 10). These microvoids are believed to result from the presence of fluorine impurity in the particle coatings which forms a volatile tungsten oxyfluoride specie at elevated temperatures (ref. 5). Coalescence of these microvoids along the tungsten grain boundaries in combination with fuel

[REDACTED]

[REDACTED]

migration into the grain boundaries (fig. 11(a)) is believed to be partially responsible for the internal cracking and the fracturing observed in cermet (fig. 9).

The notches, cavities, and voids observed in the claddings on cermets (figs. 2(d), 5, and 9) were formed during the vapor deposition process as discussed previously. Because tungsten (with which all particles were coated) is relatively insensitive to the leaching acid solution, one would not expect the surface fuel particles to have been attacked by the acid. This attack is believed to result from the formation of a tungsten-molybdenum alloy at the cermet-molybdenum interface during consolidation. This alloy is not as insensitive as tungsten to the acid solution. Evidence of alloying is presented in figure 12 where an area of little or no alloying (fig. 12(a)) is contrasted to an area in which molybdenum appears to contact the surface of fuel particles (fig. 12(b)). In addition, voids were found in the molybdenum indicating a Kirkendahl-type alloying. Electron microprobe analysis of a similar area (fig. 12(b)) indicated that an alloy was formed between the tungsten coating on the UO_2 particles and the molybdenum.

The acid attack on cermets was observed to be particularly severe in a zone along the edges of each specimen which had been exposed to acid for the longest period of time. This edge attack is illustrated by a radiograph (fig. 12(c)) which delineates an area of decreased specimen thickness along the specimen edges. As will be discussed later, this attack is believed to contribute to fracturing and to blistering of specimens. For example, it was found that the majority of fractures and blisters were located near the specimen edges (figs. 9 and 10).

As mentioned previously, notches and cavities in the tungsten cladding appeared to be associated with increased fuel loss from cermets. Several reasons for this adverse effect on the fuel retention properties of cermets may be hypothesized. First, the presence of notches or cavities decreases the distance (and thus time) through which fuel must migrate in order to reach the external surface and volatilize. Second, since cermet thickness growth was observed, the cladding was put into tension, and thus the notches could act as stress concentrators. These stress concentrations would tend to increase the depth and the width of the notches at temperature via plastic deformation and thus facilitate fuel loss. Third, as is discussed in the appendix, the very rapid heating rate during cycling could cause a considerable transient hydrogen pressure buildup to occur in the cladding cavities provided that the cavity is completely or nearly completely enclosed. This increased pressure could tend to rupture the cladding and to expose fuel to the external atmosphere.

Effects of Cycling Conditions

Hydrogen pressure. - High hydrogen pressure had several effects on the thermal cyclic behavior of cermets. It was observed that, in general, the onset of rapidly accel-

erating fuel loss occurred after a lower number of cycles and that the rate of accelerated loss was greater in high- than in low-pressure hydrogen. (See figs. 6 and 7; the onset of accelerated loss did not occur up to 50 cycles in those specimens illustrated in fig. 4.) One explanation for this effect is that a greater degree of fuel migration and fuel particle interconnection resulted from an equal number of thermal cycles in high-pressure than in low-pressure hydrogen (fig. 5). Thus, in the event of a cladding flaw, more fuel would be expected to volatilize from the defect area because more particles are interconnected. The more extensive migration in the high-pressure hydrogen environment is believed to result from more extensive reduction of UO_2 to free uranium which, in turn, determines the degree of fuel migration (ref. 9).

The relative extent of fuel migration does not, however, explain another effect of high-pressure cycling on cermet, that is, the formation of fractures and blisters. For example, even though considerable migration was found in some cermets cycled in low pressure, fractures and blisters were not observed. One possible explanation for this behavior is a transient pressure which depends upon the permeation of hydrogen into cavities and voids in the cermet and upon the rapid heating of this hydrogen during each thermal cycle. This transient pressure effect is described in detail in the appendix. It is proposed that the mechanism which causes this phenomenon consists of (1) formation of a cavity or a void in the cermet and (2) propagation of blisters or fractures from this cavity or void by pressure surges. Blisters are believed to result from plastic yielding of tungsten before fuel migration and cermet embrittlement occur while fractures result after the tungsten is embrittled because of fuel migration. If this hypothesis is correct, cermet blisters and fractures could be reduced by reducing the sources of cavities and voids. These sources include the fabrication defects previously discussed as well as fuel migration and volatilization.

Future work needs to be done to define the causes and to find the cures for fracturing and blistering of cermets thermally cycled in a high-pressure hydrogen environment. Other mechanisms, such as (1) thermal expansion differences between tungsten and the migrated fuel and (2) formation of gases from impurities which exert high internal pressures (e.g., CH_4 , UF_4) may also contribute to cermet blistering and fracturing. Such future work should emphasize quality control during fabrication to minimize cladding and cermet defects and impurities.

Peak cycling temperature and time at temperature per cycle in high-pressure hydrogen. - As mentioned previously, increasing the thermal cycling temperature from 2500° to 2600° C resulted in increased fuel migration and loss. (Compare fig. 4 with fig. 6.) This increase is in agreement with the results of other studies on similar specimens (produced from uncoated particles) reported in reference 9. The high-pressure hydrogen environment not only caused increased fuel migration in cermets cycled to 2600° C, but it resulted in a high percentage of fractured specimens. These fractures, which resulted in

CONFIDENTIAL

catastrophic fuel loss, are believed to be due to extensive fuel migration which embrittled the tungsten matrix. These observations indicate that reactor temperature excursions or fuel element hot spots, which cause fuel elements to heat to temperatures approaching 2600°C in high-pressure hydrogen, may have a disastrous effect on reactor lifetime and performance.


Cermets cycled to 2500°C for 1 hour per cycle exhibited more fuel migration and loss per cycle than cermets cycled to 2500°C for 10-minute cycles. The frequency of specimens which fractured during 1-hour cycles to 2500°C was higher than for 10-minute cycles to 2500°C but lower than for 10-minute cycles to 2600°C (in high-pressure hydrogen). The relative frequency of fractures was found to correspond with the relative extent of fuel migration and, therefore, the extent of tungsten embrittlement. The relative frequency of blistered specimens, on the other hand, would not be expected to be higher on specimens cycled under conditions which increase the rate of fuel migration because blisters are believed to form before the tungsten is embrittled. This expectation was realized as may be seen in table IV, which illustrates that the frequency of blistered specimens was not significantly changed as either peak cycling temperature or time at temperature per cycle was increased.

CONCLUDING REMARKS

The fuel-retention capability of cermets containing 18-mole-percent CeO_2 in UO_2 appeared to be superior to that of cermets containing 10-mole-percent of Y_2O_3 in UO_2 (at equal metal oxide cation to uranium ratios) for the majority of thermal cycling conditions studied. However, scatter in fuel loss data due to fabrication defects overshadowed the differences between the additives and makes any conclusions on the relative effectiveness of the additives somewhat questionable. The large degree of scatter in fuel loss data observed between specimens at all thermal cycling conditions is indicative of uncontrolled variables in specimen fabrication. These variables must be controlled in order to ensure reliable and consistent thermal cyclic fuel retention performance of fuel elements in a nuclear rocket.

SUMMARY OF RESULTS

Cermet specimens were fabricated by hot isostatic compaction of tungsten-coated UO_2 particles (nominally W - 35-volume-percent UO_2 containing 18-mole-percent CeO_2 or 10-mole-percent Y_2O_3 in the UO_2) followed by complete encapsulation of the consolidated cermets with vapor deposited tungsten. These specimens exhibited the following properties upon thermal cycling in dry, flowing hydrogen:


1. Specimens containing either CeO_2 or Y_2O_3 in the UO_2 were capable of meeting the fuel retention goal of less than 1 percent of fuel loss after twenty-five 10-minute cycles to 2500°C in either 15 or 600 psia (0.10 or 4.1 MN/m^2) of hydrogen.

2. Fuel loss from specimens began to accelerate after a lower number of thermal cycles when either the peak cycling temperature or time at temperature per cycle were increased from those conditions previously indicated.

3. Thermal cycling in 600 psia (4.1 MN/m^2) of hydrogen had, in general, more severe effects on the specimens than did testing in 15 psia (0.10 MN/m^2) of hydrogen. In particular, blistering and/or gross fracturing and more extensive fuel migration of some specimens were observed after high-pressure testing. A significantly higher frequency of fractured specimens was observed when specimens were cycled to 2600°C in 600 psia (4.1 MN/m^2) of hydrogen than for any other set of test conditions used in this study.

Lewis Research Center,
National Aeronautics and Space Administration,
Cleveland, Ohio, April 13, 1967,
122-28-01-01-22.

APPENDIX - TRANSIENT PRESSURE EFFECT

A proposed explanation for the occurrence of fractures and blisters as well as the higher rate of fuel loss (once fuel loss begins to accelerate in high-pressure hydrogen) is that of a transient internal pressure resulting from the presence of hydrogen in specimen voids (not connected to the external surface) and cavities (connected to the external surface by an extremely fine channel). As mentioned previously, voids and cavities in the cladding on a cermet were formed during fabrication (fig. 2(d)) while matrix microvoids were formed in the cermet during thermal cycling (figs. 7, 9, and 10). In addition, cermet cavities were formed by fuel migration through the cladding (fig. 11(b)) and subsequent volatilization of fuel particles exposed to the atmosphere. It is proposed that hydrogen entered cavities through their channels to the external surface and permeated through tungsten into voids as a monatomic specie. The permeation of hydrogen through tungsten has been shown to be significant at 2500°C and to increase with an increased hydrogen pressure differential and with increased temperature and time at temperature (ref. 14). In addition, monatomic hydrogen may enter voids during cooling because of dissolution of hydrogen from tungsten. (See refs. 14 and 15 for solubility of hydrogen in tungsten.) Essentially all the monatomic hydrogen in the voids would be expected to form molecular hydrogen during cooling (ref. 15).

Once hydrogen is present in a cavity or void, rapid heating (from 25° to 2500°C) will increase its pressure approximately nine times assuming no hydrogen escapes. Assuming that the pressure in the voids and cavities was equal to the external pressure before heating began, heating would cause a substantial pressure differential with the constantly regulated external pressure employed in this study. For example, if the external pressure was 15 or 600 psia (0.10 or 4.1 MN/m^2), the internal pressure could increase to a maximum of 135 or 5400 psia (0.92 or 37.2 MN/m^2) and result in a maximum net pressure differential of 120 or 4800 psia (0.82 or 33.1 MN/m^2), respectively. It is estimated that the strength of the tungsten matrix is about 2000 psia (13.8 MN/m^2) based on data for similarly fabricated cermet specimens (ref. 11). Thus, it may be seen that the 600 psia (4.1 MN/m^2) external pressure, but not the 15 psia (0.10 MN/m^2) pressure could potentially fracture the specimen.

Admittedly, the maximum pressure differential calculated will not be achieved because of escape of hydrogen gas from cavities and voids during heating. Hydrogen gas would be expected to expand and to escape from a cavity during heating at a rate depending upon the size of the cavity opening and upon the heating rate. Unless this opening was extremely fine (submicron), no pressure buildup in the cavity would be expected. On the other hand, the rate of escape of hydrogen gas from internal voids by permeation through tungsten is expected to remain very low until the temperature is sufficiently increased. For example, very limited permeation of hydrogen through tungsten was observed below

CONFIDENTIAL

1500⁰ C (ref. 14). Thus, the hydrogen pressure in voids would be expected to increase at least six times during heating (since the absolute temperature has increased six times at 1500⁰ C) before a significant amount of hydrogen escapes. In summary, the maximum pressure in either cavities or voids (nine-fold at 2500⁰ C) would not be reached, and the pressure achieved would be transient as the internal and external pressures equalize at high temperature.

The assumption that the internal and external pressures are equal at ambient temperatures after the specimen has experienced thermal cycling is also somewhat questionable. The pressure in cavities may be equal to the external pressure because of the channels to the atmosphere. The internal pressure in voids, however, would depend upon the net permeation of hydrogen into voids which is dependent upon the extent of dissociation, diffusion, solution, and dissolution of hydrogen in tungsten during a given thermal cycle. It may be calculated that any internal hydrogen pressure greater than 67 psia (0.46 MN/m²) at ambient temperature will result in a pressure greater than a 600 psia (4.1 MN/m²) external pressure upon rapid heating to 2500⁰ C provided hydrogen is not lost during heating.

While the extent of a transient pressure effect on deteriorating specimens and thereby increasing fuel loss is not quantitatively known, it is believed that the following factors would increase this effect: (1) a higher external pressure, (2) a higher cycling temperature, (3) an increased number and volume of cavities and voids resulting from fabrication, (4) an increased number and volume of microvoids generated in the tungsten matrix of the cermet during thermal cycling, (5) increased fuel migration which results in more and larger cavities where fuel is volatilized, and (6) a decreased cavity opening size to the atmosphere which would reduce the rate of hydrogen loss.



REFERENCES

1. Krasner, Morton H.: A Reference Design for the Tungsten Water-Moderated Nuclear Rocket. Nuclear Rocket Technology Conference. NASA SP-123, 1966, pp. 159-173.
2. Gedwill, Michael A.; Sikora, Paul F.; and Caves, Robert M.: Fuel-Retention Properties of Tungsten-Uranium Dioxide Composites. NASA TM X-1059, 1965.
3. Garfinkle, Margin: Effect of Additives on Thermal Stability of Tungsten-Uranium Dioxide Composites. NASA TM X-1118, 1965.
4. Gedwill, Michael A.: An Investigation of Some Variables Affecting and Methods of Inhibiting Thermal-Cyclic Fuel Losses from Tungsten-Uranium Dioxide Composites. NASA TM X-1296, 1966.
5. Watson, Gordon K.; Caves, Robert M.; and Saunders, Neal T.: Preparation and Roll Compaction of Tungsten-Coated Uranium Dioxide Particles. NASA TM X-1448, 1967.
6. Caves, Robert M.: Evaluation of Vapor Deposited Tungsten Claddings on Tungsten - Uranium Dioxide (W-UO₂) Composites. NASA TM X-1449, 1967.
7. Sikora, Paul F.; and Blankenship, Charles P.: Evaluation of Tungsten-Uranium Dioxide Honeycomb Structures. NASA TM X-1445, 1967.
8. Gluyas, Richard E.; and Gedwill, Michael A.: Stabilization of Tungsten-Uranium Dioxide Composites under Thermal Cycling Conditions. NASA TM X-1295, 1966.
9. Takkunen, Philip D.; Gluyas, Richard E.; and Gedwill, Michael A.: Thermal Cyclic Behavior of Tungsten-Uranium Dioxide Cermets Containing Metal Oxide Additives. NASA TM X-1446, 1967.
10. Baker, R. J.; Daniel, J. L.; Lackey, W. J.; Lobsinger, R. J.; Scott, S. A.; Snajdr, E. A.; and Roake, W. E.: Basic Behavior and Fuel Retention Properties of Tungsten-Uranium Dioxide Cermets. Rep. No. BNWL-CC873 (NASA CR-54840), Battelle-Northwest, 1967.
11. Buzzard, Robert J.: Factors Affecting the High-Temperature Strength of Tungsten - Uranium Dioxide Composites. NASA TM X-1444, 1967.
12. Goetsch, G. R.; Cover, P. W.; Gripshover, P. J.; Wilson, W. J.; and Boyer, C. B.: Fabrication of Tungsten-UO₂ Hexagonal-Celled Fuel-Element Configurations. Battelle Memorial Institute (NASA CR-54796), Oct. 30, 1965.
13. Grisaffe, Salvatore J.; and Caves, Robert M.: Fuel Retention Improvement at High Temperatures in Tungsten-Uranium Dioxide Dispersion Fuel Elements by Plasma-Spray Cladding. NASA TM X-1028, 1964.

14. Aitken, E. A.; Conn, P. K.; Duderstadt, E. C.; and Fryxell, R. E.: Measurement of the Permeability of Tungsten to Hydrogen and to Oxygen. General Electric Co. (NASA CR-54918), May 1966.
15. Moore, George E.; and Unterwald, F. C.: Thermal Dissociation of Hydrogen. J. Chem. Phys., vol. 40, no. 9, May 1, 1964, pp. 2639-2652.

CONFIDENTIAL

TABLE I. - ANALYSIS OF UO_2 PARTICLES BEFORE AND AFTER COATING
WITH VAPOR DEPOSITED TUNGSTEN

Property	UO_2 - 10-mole-percent Y_2O_3 particles		UO_2 - 18-mole-percent CeO_2 particles	
	Uncoated	Tungsten coated	Uncoated	Tungsten coated
Mole percent of additive in UO_2	10.0	-----	18.2	-----
Lattice constant of FCC structure, Å	^a (5.462)	-----	(5.459)	-----
Volume percent of UO_2 in W	-----	34.9	-----	34.5
Volume percent of ceramic in W	-----	41.7	-----	42.6
Percent of theoretical densities of particles	99.7	(99.9)	93.2	(98.3)
Percent of theoretical densities of consolidated particles	-----	(99.4)	-----	(98.5)
Element for trace analysis	Concentration, ppm			
Al	80	<25	100	40
B	<5	<25	<5	<25
Be	<10	<25	<10	<25
C	28	12 (<1)	60	<10 (4)
Cl ^b	<10	15 (17)	<10	18 (43)
Co	<5	<25	<5	<25
Cr	<10	<25	10	<25
Cu	<6	<25	<6	<25
F	<10	56 (107)	16	43 (80)
Fe	<20	35	<20	50
Mg	<10	<25	<10	<25
Mn	<10	<25	<10	<25
Mo	100	<25	<10	<25
N	<10	<10 (22)	15	38 (53)
Ni	<10	<25	<10	<25
Pb	25	-----	2	-----
S	<10	14 (2)	<10	<10 (4)
Si	<25	<50	<50	<50
Sn	<2	<25	2	<25
Ti	<5	<25	<10	<25
V	<5	<25	10	<25
Zr	40	25	100	<25

^aAnalyses given in parenthesis were obtained from an independent laboratory; all other analyses were obtained from material vender.

^bCl analyzed as total halogens other than F.

CONFIDENTIAL

TABLE II. - COMPARISON OF FURNACE OPERATING CHARACTERISTICS

Furnace location	Lewis Research Center (NASA)	Battelle Northwest Laboratory	
Furnace volume, cu ft (m ³)	0.026 (0.74×10 ⁻³)	0.31 (8.9×10 ⁻³)	
Hydrogen pressure, psia (MN/m ²)	15 (0.10)	15 (0.10)	600 (4.1)
Hydrogen:			
Flow, standard cu ft/hr (m ³ /hr)	35 (1)	35 (1)	35 (1)
Oxygen impurity, ppm	<10	<10	<10
Water impurity, ppm	<10	<10	<10
Temperature, °C			
Accuracy ^a	±20	±15	±15
Gradient ^b	-----	<10	<10
Heating rate to 2500° C, °C/sec	32	22	22
Cooling rate, °C/sec			
2500° to 800° C	37 - 40	9 - 12	14
800° to 500° C	9 - 14	3 - 7	7
500° to 200° C	2 - 6	1 - 3	3

^aCalibrated pyrometers were sighted on blackbody hole.

^bTemperature gradient across specimen holder was insignificant in either furnace based on program which varied position of specimens in holder. Absolute temperatures were also determined at BNW by checking melting points of pure Mo and Nb inserted in furnace.

TABLE III. - SUMMARY OF EFFECT OF TIME AT TEMPERATURE

PER CYCLE ON FUEL LOSS

Cycling conditions			Additive in UO ₂			
			18-mole-percent CeO ₂		10-mole-percent Y ₂ O ₃	
Hydrogen pressure	Time at 2500° C per cycle, min	Number of cycles to 2-weight-percent fuel loss	Total time at temperature for 2-weight-percent loss, hr	Number of cycles to 2-weight-percent fuel loss	Total time at temperature for 2-weight-percent loss, hr	
psia	MN/m ²					
15	0.10	10	102	17	36	6
		60	21	21	9	9
		120	20	40	9	18
600	4.1	10	48	8	54	9
		60	8	8	8	8

TABLE IV. - FREQUENCY OF FRACTURED AND BLISTERED SPECIMENS
RESULTING FROM THERMAL CYCLING

Cycling conditions				Total number of specimens tested	Specimens exhibiting visible fractures, percent	Specimens exhibiting visible blisters, percent
Pressure at 35 standard cu ft/hr (1.0 m ³ /hr)		Temperature, °C	Time at temperature per cycle, min			
psia	MN/m ²					
15	0.10	2500	10	19	0	0
		2500	60	4	↓	↓
		2500	120	7		
		2600	10	4	↓	↓
600	4.1	2500	10	16	6	25
		2500	60	6	50	33
		2600	10	8	75	25

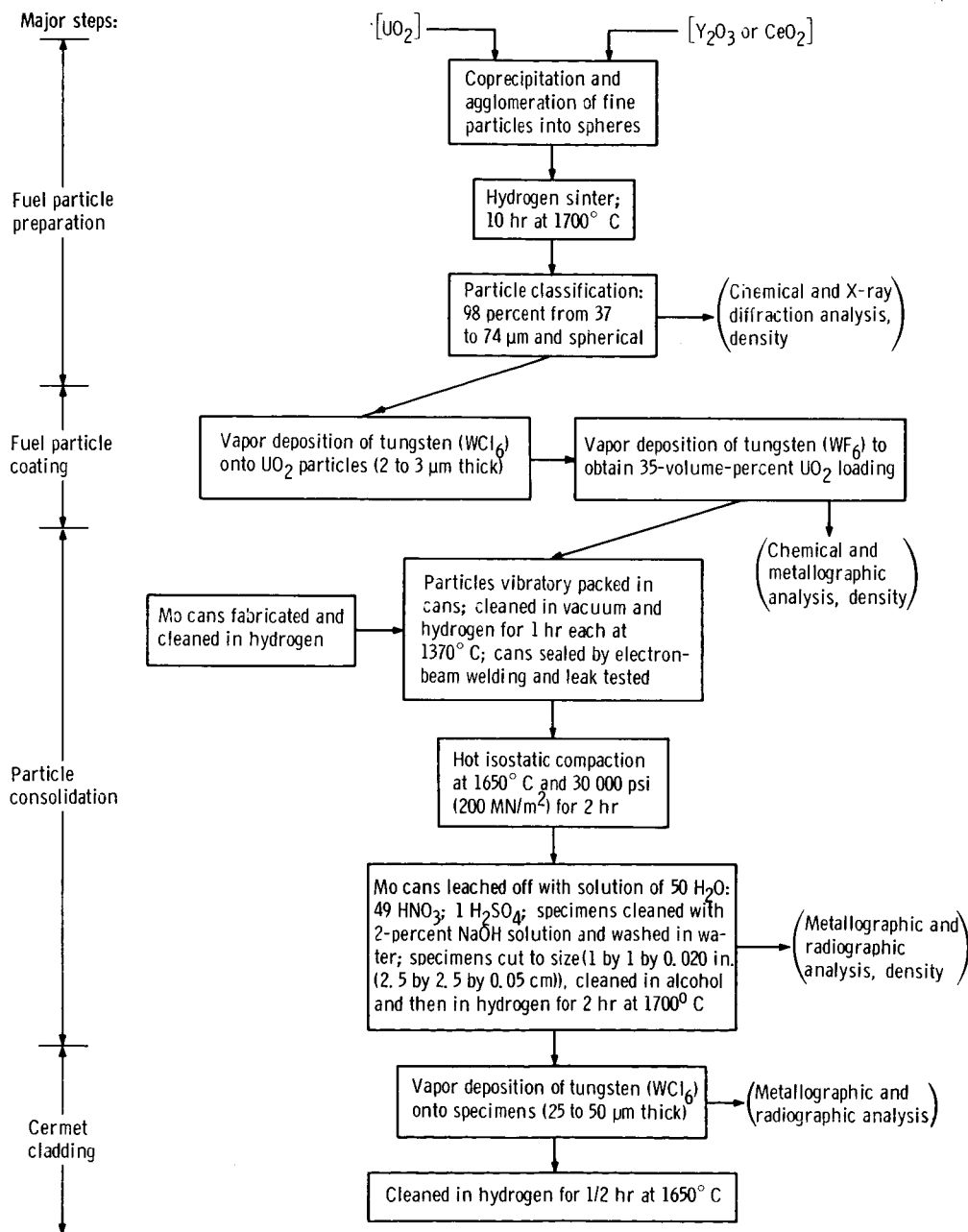
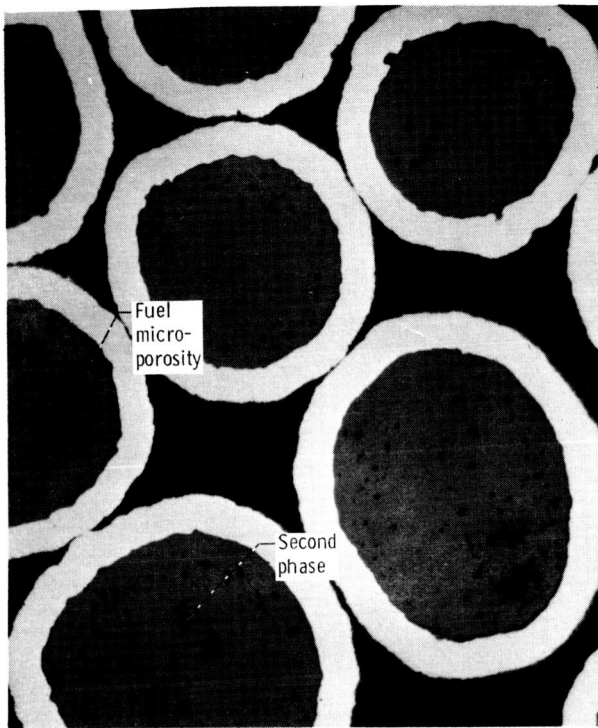
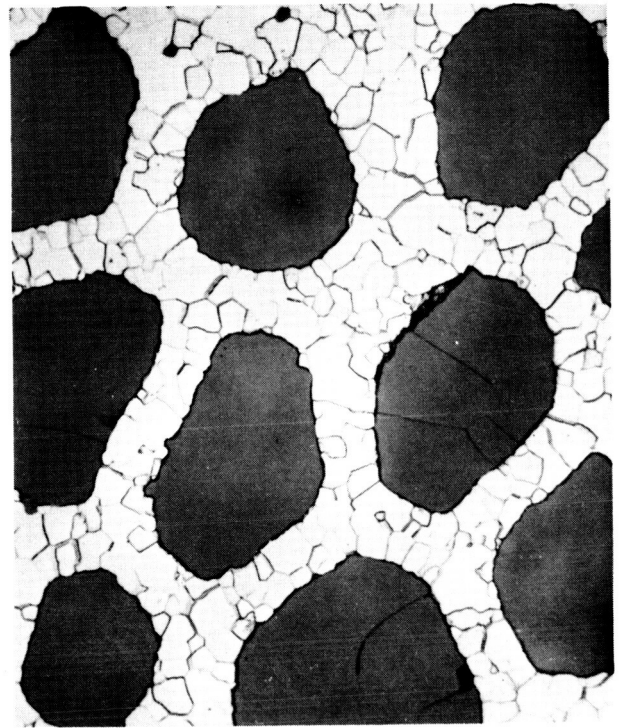


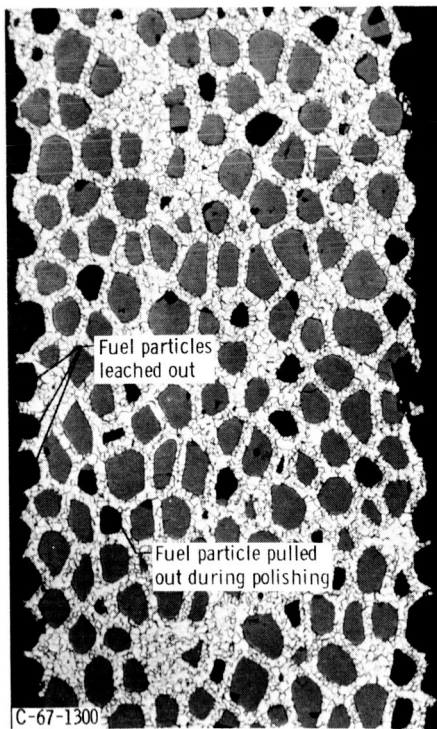
Figure 1. - Flow chart of specimen preparation.



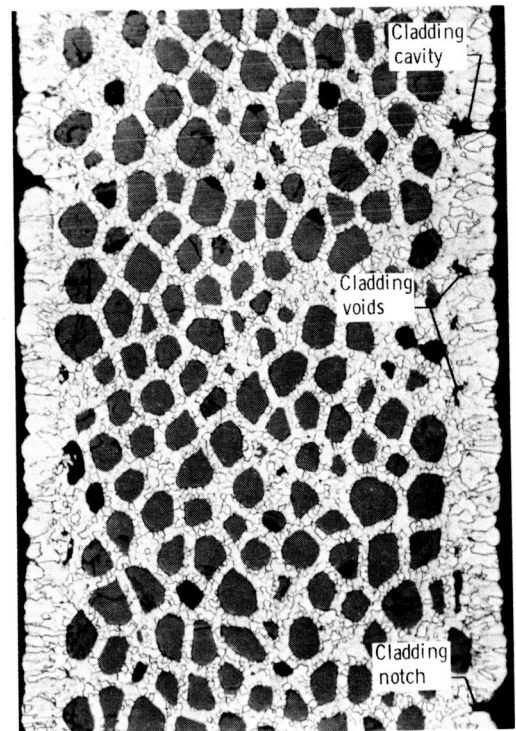
(a) Tungsten-coated fuel particles. Unetched; X500.



(b) Hot isostatically consolidated particles. Etched; X500.



(c) Consolidated cermet after acid leaching. Etched; X100.



(d) Consolidated cermet after leaching and cladding. Etched; X100.

Figure 2. - Microstructures of tungsten-UO₂ particles and cermets after the following fabrication steps: particle preparation, cermet consolidation, cermet leaching, and cermet cladding.

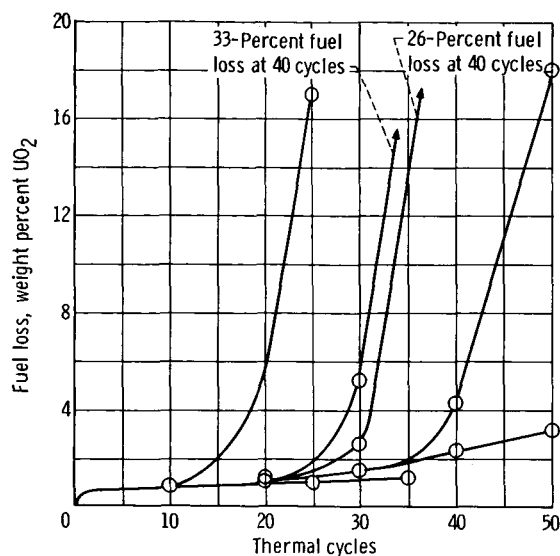


Figure 3. - Scatter in thermal cyclic induced fuel loss from fully clad tungsten - 35-volume-percent UO_2 cermet containing 10-mole-percent Y_2O_3 in UO_2 . 10-Minute cycles to 2500°C in hydrogen at 15 psia (0.10 MN/m^2) and 35 standard cubic feet per hour (1.0 m^3/hr).

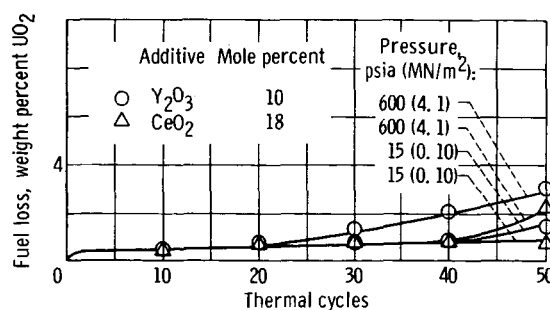
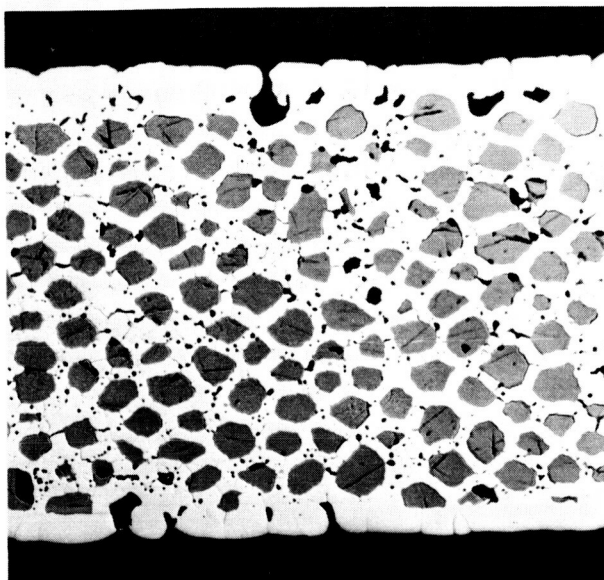
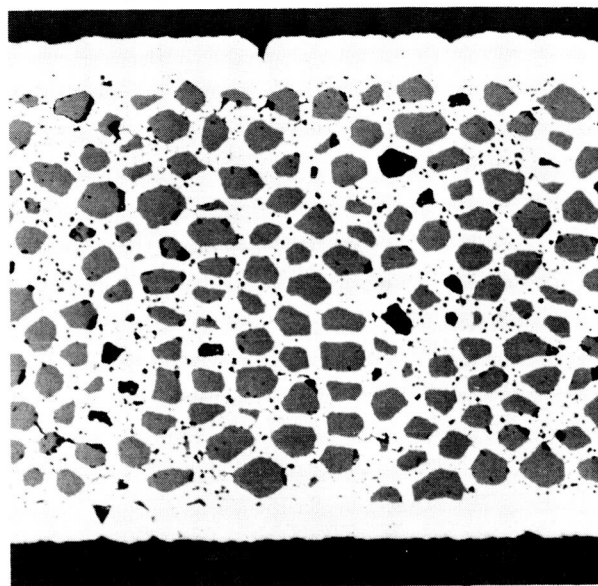


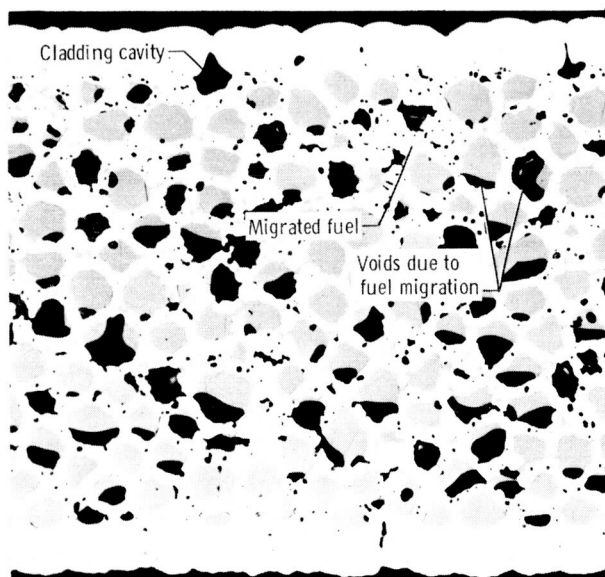
Figure 4. - Effect of hydrogen pressure at 2500°C on thermal cyclic induced fuel loss from fully clad tungsten - 35-volume-percent UO_2 cermet containing the indicated oxide in UO_2 . 10-Minute cycles to 2500°C in hydrogen at indicated pressure and 35 standard cubic feet per hour (1.0 m^3/hr).



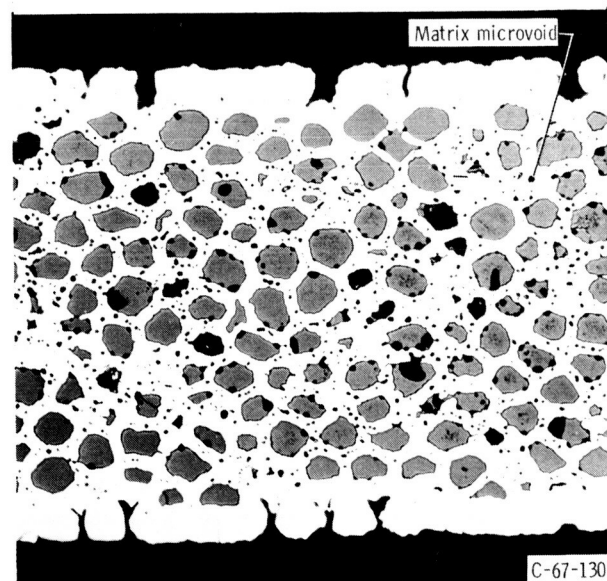
(a) 10-Mole-percent Y_2O_3 ; cycled at 15 psia (0.10 MN/m^2) with 3.1-weight-percent fuel loss.



(b) 18-Mole-percent CeO_2 ; cycled at 15 psia (0.10 MN/m^2) with 1.0-weight-percent fuel loss.



(c) 10-Mole-percent Y_2O_3 ; cycled at 600 psia (4.1 MN/m^2) with 1.4-weight-percent fuel loss.



(d) 18-Mole-percent CeO_2 ; cycled at 600 psia (4.1 MN/m^2) with 2.4-weight-percent fuel loss.

Figure 5. - Microstructures illustrating effect of hydrogen pressure on fully clad tungsten - 35-volume-percent- UO_2 cermets containing Y_2O_3 or CeO_2 in UO_2 . Fifty 10-minute cycles to 2500°C in hydrogen at indicated pressure and 35 standard cubic feet per hour ($1.0 \text{ m}^3/\text{hr}$). Unetched; X100.

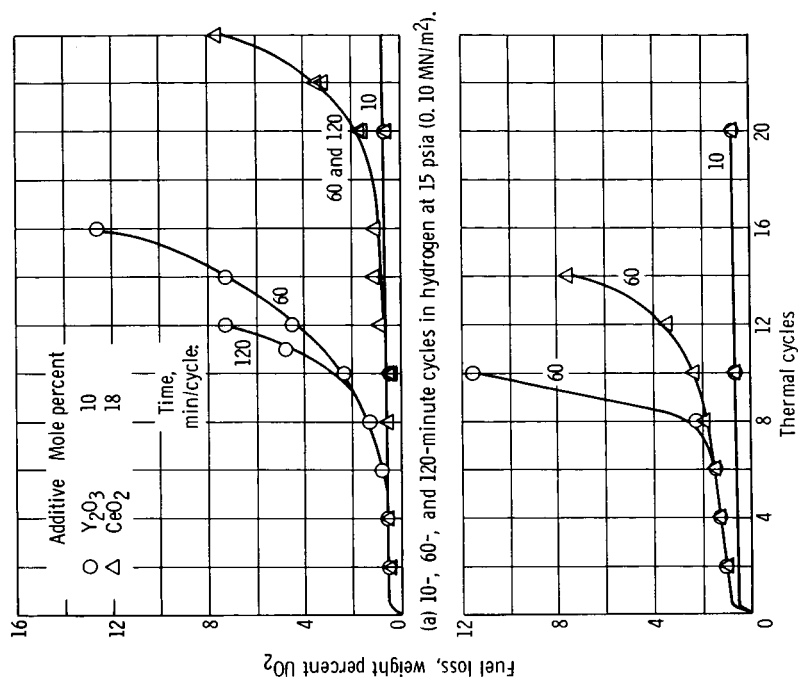
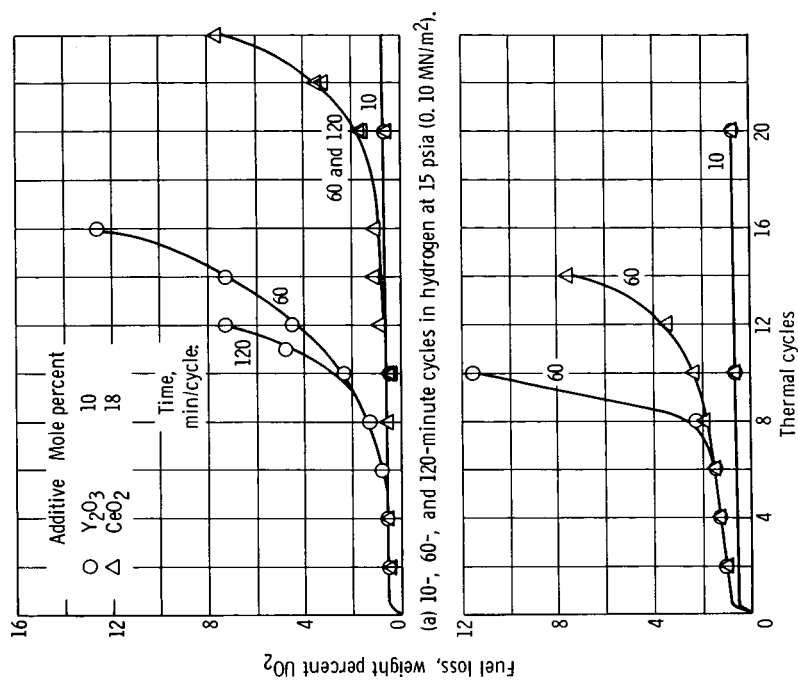


Figure 6. - Effect of hydrogen pressure at 2600° C on thermal cyclic induced fuel loss from fully clad tungsten - 35-volume-percent- UO₂ cermet containing indicated oxide in UO₂. 10-Minute cycles to 2600° C in hydrogen at indicated pressure and 35 standard cubic feet per hour (1.0 m³/hr).



(b) 10- and 60-minute cycles in hydrogen at 600 psia (4.1 MN/m²).
Figure 7. - Effect of time at temperature per thermal cycle on fuel loss from fully clad tungsten - 35-volume-percent-UO₂ cermet containing indicated oxide in UO₂. Cycled to 2500° C in hydrogen at 35 standard cubic feet per hour (1.0 m³/hr).

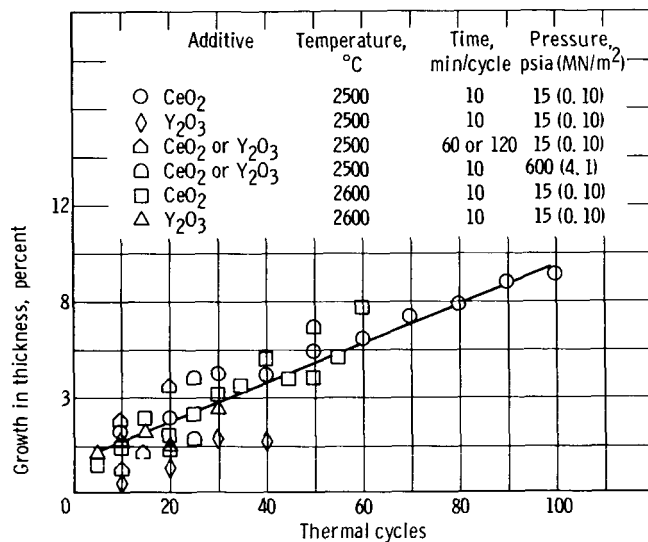
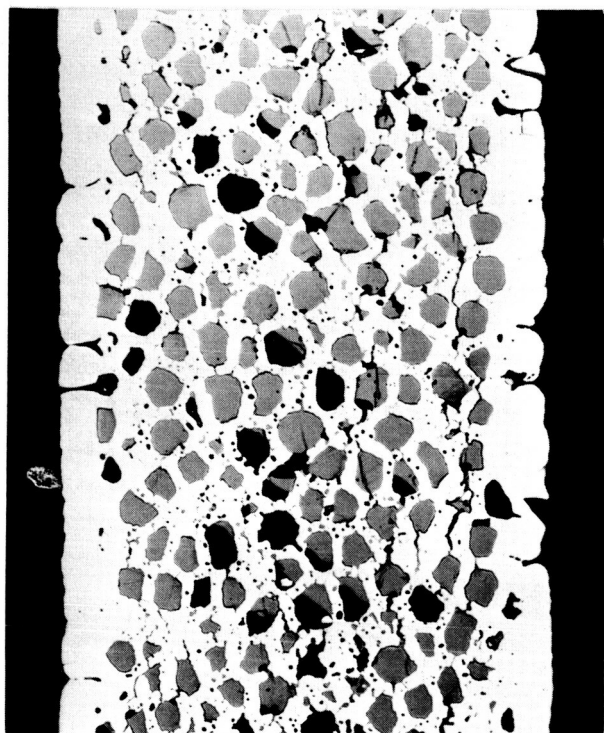
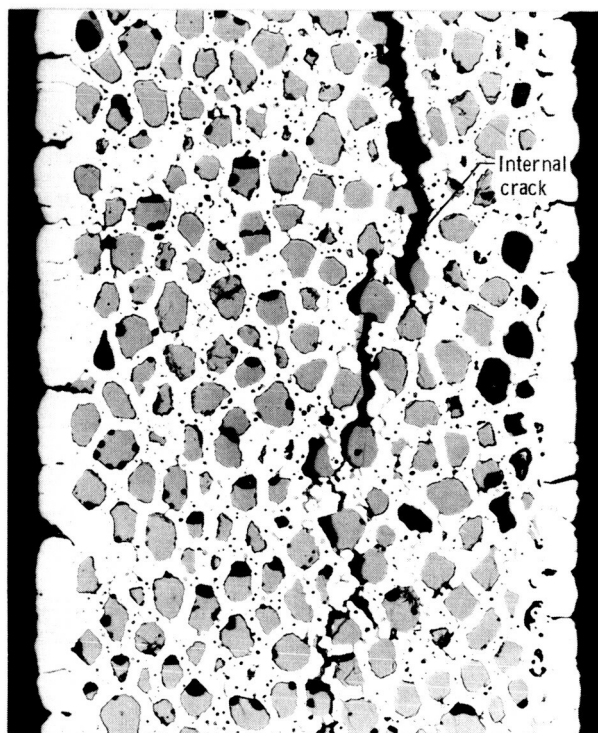


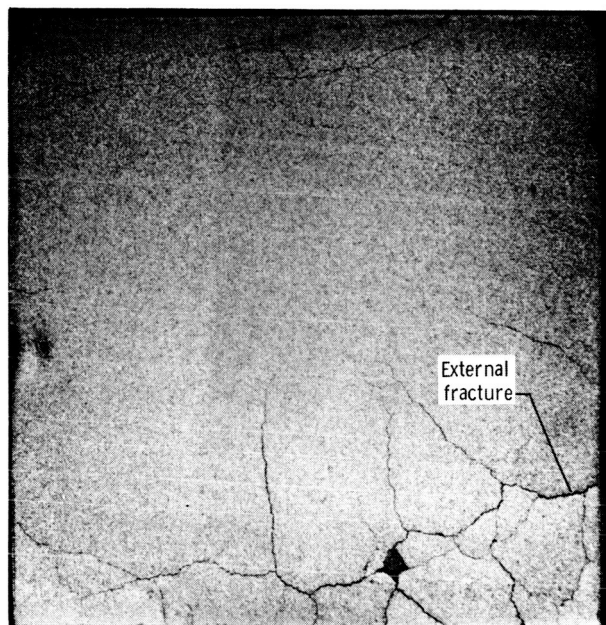
Figure 8. - Thermal cyclic induced dimensional growth of fully clad tungsten - 35-volume-percent-UO₂ cermets containing 18-mole-percent CeO₂ of 10-mole-percent Y₂O₃ in UO₂. Cycled in hydrogen at 35 standard cubic feet per hour (1.0 m³/hr) and at indicated pressure, time, and temperature.



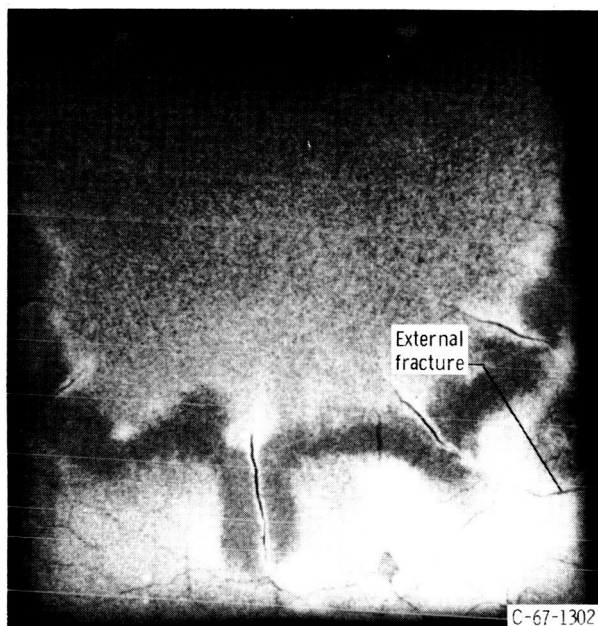
(a) 18-Mole-percent CeO_2 ; 50 cycles to 2500°C with 5.6-weight-percent fuel loss. Unetched; X100.



(b) 10-Mole-percent Y_2O_3 ; 50 cycles to 2500°C with 8.5-weight-percent fuel loss. Unetched; X100.



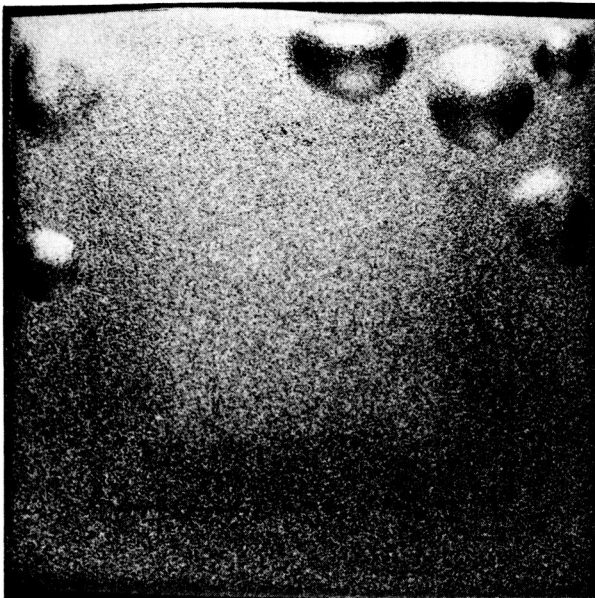
Macrograph



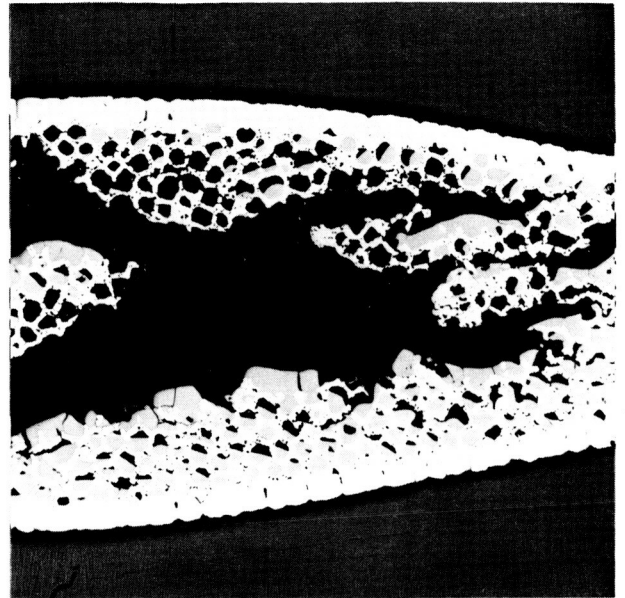
Radiograph

(c) CeO_2 ; 10 cycles to 2600°C with 57.0-weight-percent fuel loss; X3.

Figure 9. - Thermal cyclic induced fracturing of fully clad tungsten - 35-volume-percent UO_2 cermet containing Y_2O_3 or CeO_2 in the UO_2 . 10-Minute cycles to indicated temperature in hydrogen at 600 psia (4.1 MN/m^2) and 35 standard cubic feet per hour ($1.0\text{ m}^3/\text{hr}$).

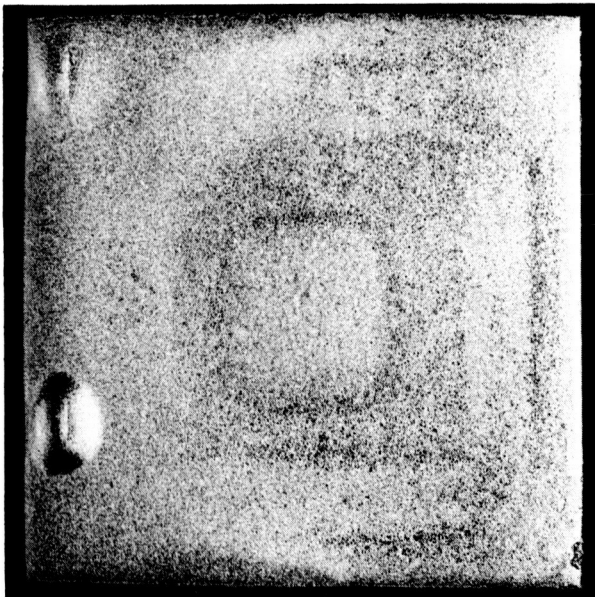


Macrograph, X3

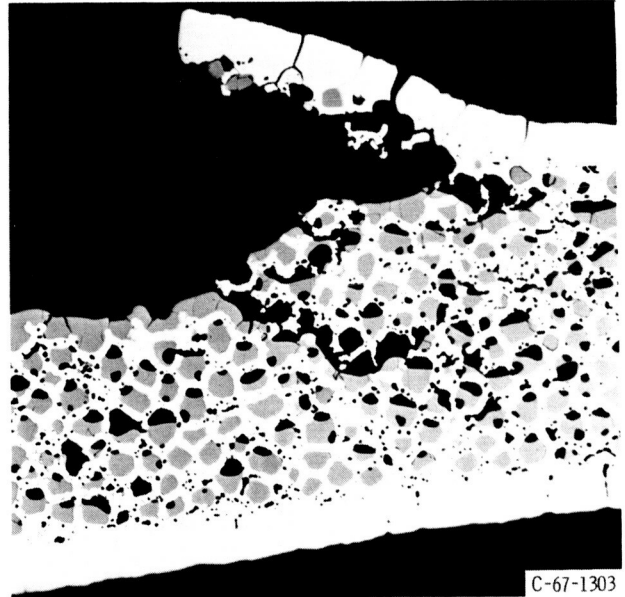


Micrograph, unetched; X50

(a) 10-Mole-percent Y_2O_3 , 1.4-weight-percent fuel loss.



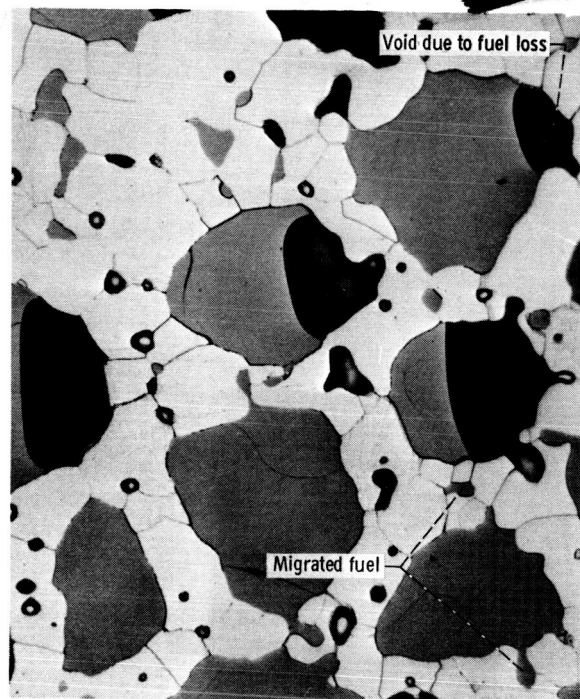
Macrograph, X3



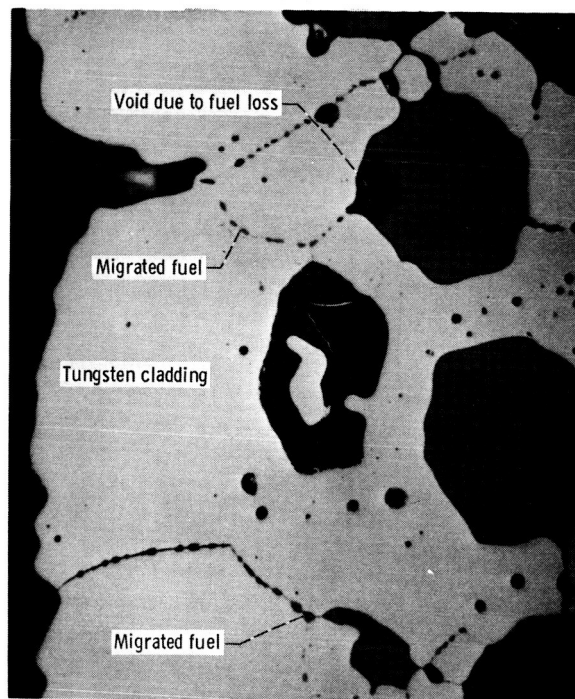
Micrograph, unetched; X50

(b) 18-Mole-percent CeO_2 ; 5.6-weight-percent fuel loss.

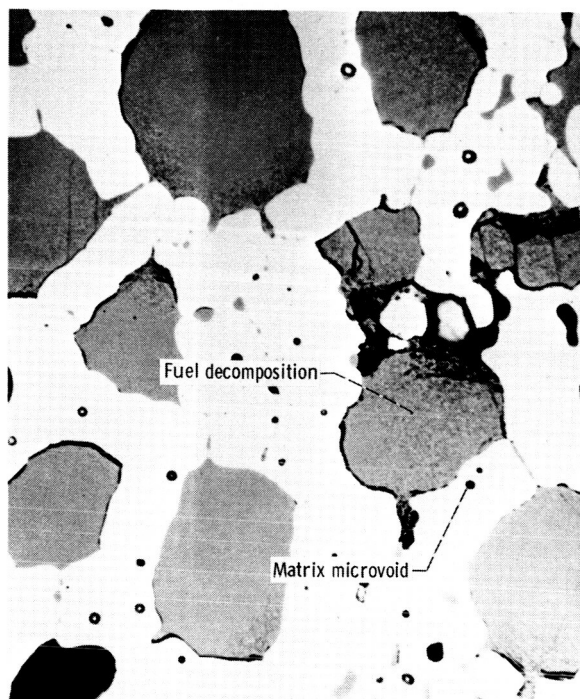
Figure 10. - Thermal cyclic induced blistering of fully clad tungsten - 35-volume-percent- UO_2 cermets containing Y_2O_3 or CeO_2 in UO_2 . Fifty 10-minute cycles to 2500° C in hydrogen at 600 psia (4.1 MN/m²) and 35 standard cubic feet per hour (1.0 m³/hr).



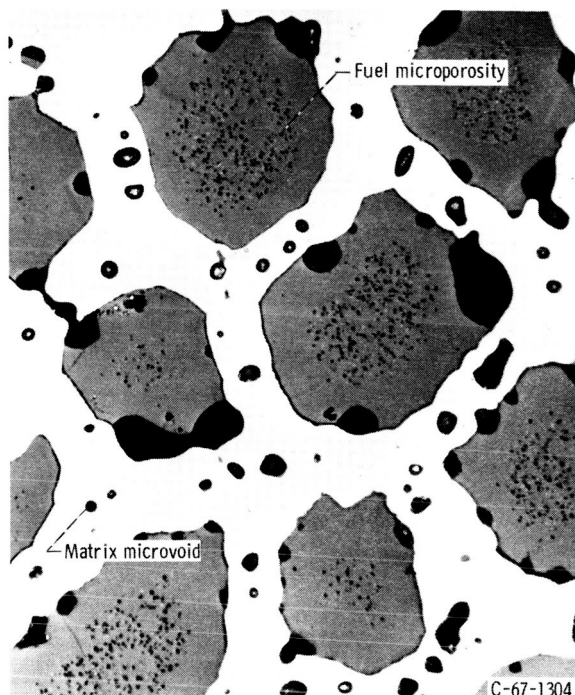
(a) 10-Mole-percent Y_2O_3 ; cycled at 600 psia (4.1 MN/m²) with 1.4-weight-percent fuel loss. Etched.



(b) 10-Mole-percent Y_2O_3 ; cycled at 15 psia (0.10 MN/m²) with 17.9-weight-percent fuel loss. Unetched.

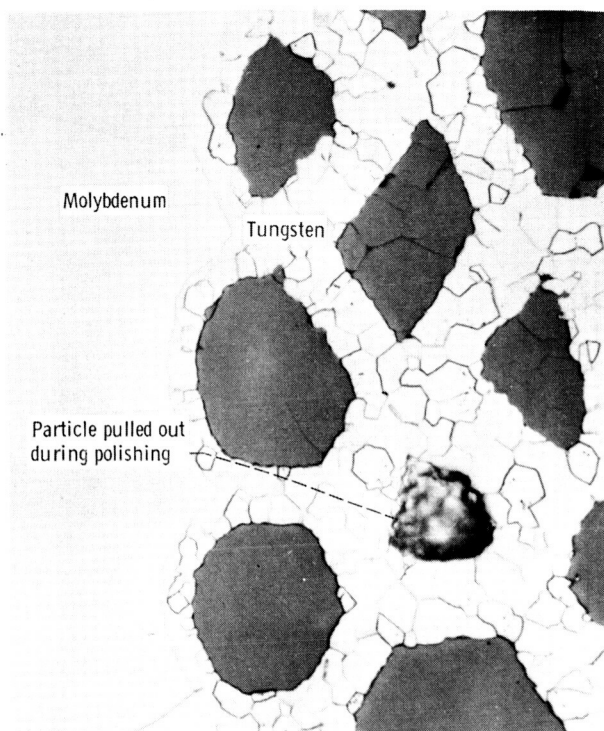


(c) 18-Mole-percent CeO_2 ; cycled at 600 psia (4.1 MN/m²) with 5.6-weight-percent fuel loss. Unetched.

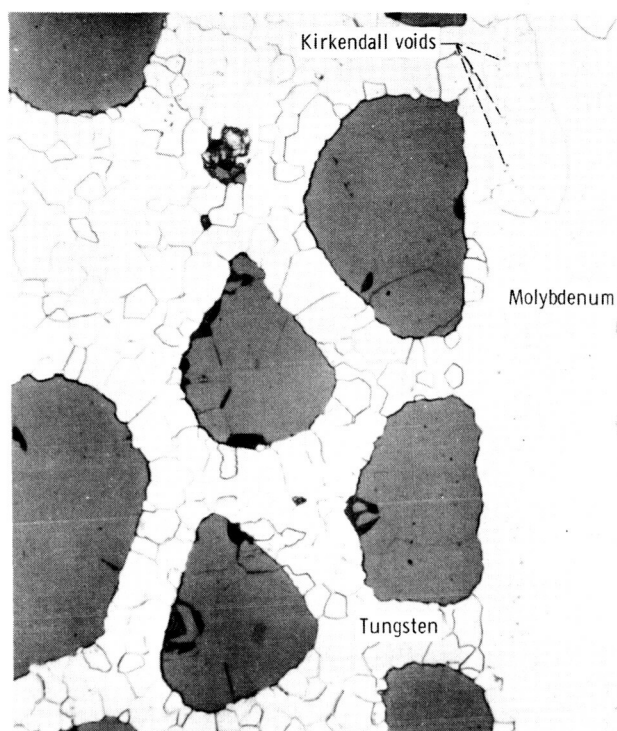


(d) 10-Mole-percent Y_2O_3 ; cycled at 600 psia (4.1 MN/m²) with 3.8-weight-percent fuel loss. Unetched.

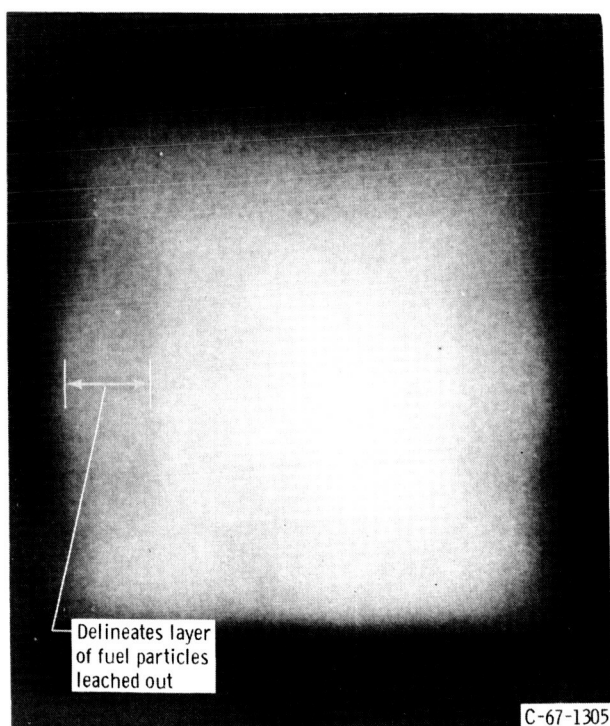
Figure 11. - Characterization of fuel migration and decomposition of thermally cycled fully clad tungsten - 35-volume-percent- UO_2 cermets containing Y_2O_3 or CeO_2 in UO_2 . Fifty 10-minute cycles to 2500° C in hydrogen at the indicated pressure and 35 standard cubic feet per hour (1.0 m³/hr).



(a) Molybdenum-cermet interface with no reaction. Etched; X500.



(b) Molybdenum interface with plastically deformed particles and W-Mo alloying. Etched; X500.



(c) Radiograph typical of acid leaching effects; X3.

Figure 12. - Micrographs and radiograph of tungsten- UO_2 cermet illustrating potential fabrication problems which can effect the behavior of cermet during thermal cycling.

[REDACTED]

"The aeronautical and space activities of the United States shall be conducted so as to contribute . . . to the expansion of human knowledge of phenomena in the atmosphere and space. The Administration shall provide for the widest practicable and appropriate dissemination of information concerning its activities and the results thereof."

—NATIONAL AERONAUTICS AND SPACE ACT OF 1958

NASA SCIENTIFIC AND TECHNICAL PUBLICATIONS

TECHNICAL REPORTS: Scientific and technical information considered important, complete, and a lasting contribution to existing knowledge.

TECHNICAL NOTES: Information less broad in scope but nevertheless of importance as a contribution to existing knowledge.

TECHNICAL MEMORANDUMS: Information receiving limited distribution because of preliminary data, security classification, or other reasons.

CONTRACTOR REPORTS: Scientific and technical information generated under a NASA contract or grant and considered an important contribution to existing knowledge.

TECHNICAL TRANSLATIONS: Information published in a foreign language considered to merit NASA distribution in English.

SPECIAL PUBLICATIONS: Information derived from or of value to NASA activities. Publications include conference proceedings, monographs, data compilations, handbooks, sourcebooks, and special bibliographies.

TECHNOLOGY UTILIZATION PUBLICATIONS: Information on technology used by NASA that may be of particular interest in commercial and other non-aerospace applications. Publications include Tech Briefs, Technology Utilization Reports and Notes, and Technology Surveys.

Details on the availability of these publications may be obtained from:

SCIENTIFIC AND TECHNICAL INFORMATION DIVISION
NATIONAL AERONAUTICS AND SPACE ADMINISTRATION

Washington, D.C. 20546

[REDACTED]